Phase diffusion in the vicinity of an oscillatory secondary bifurcation

F. Giorgiutti,* L. Limat, and J. E. Wesfreid
Laboratoire de Physique et Mécanique des Millieux Hétérogènes, CNRS URA No. 857, ESPCI, 10 rue Vauquelin, 75231 Paris Cedex 05, France

(Received 17 March 1997; revised manuscript received 29 October 1997)

The phase dynamics of a one-dimensional cellular pattern is studied on a regular array of liquid columns formed below an overflowing horizontal cylinder. When a uniform wavelength dilation is imposed by static boundaries, an oscillatory secondary bifurcation is observed (''optical mode''). The case of a moving boundary (sinusoidal motion) allows us to observe three dynamical states: phase diffusion, phase diffusion coupled with the oscillatory state, and propagation of dilation waves. The dependence of the phase diffusion coefficient D upon the pattern wavelength is investigated for different flow rates: D is nearly constant until the appearance of the oscillations and jumps to a larger value when the optical mode is excited. This unusual behavior is recovered by an analytical treatment of Coullet-Ioss equations. [S1063-651X(98)12002-0]

PACS number(s): 47.20.Ma, 47.20.Ky, 47.54.+r

I. INTRODUCTION

The dynamics of one-dimensional cellular patterns generated by instabilities have motivated various studies [1]. We can mention as examples the following systems: Rayleigh-Bénard convection [2], ''printer's experiment'' (directional viscous fingering) [3], and directional solidification [4]. A concept of central importance in the description of this dynamics is the spatial phase of the pattern [5]. In its simplest sense this quantity $\phi(x,t)$ can be defined as the local displacement of the cells δu with respect to a base state normalized by a reference wavelength λ as

$$\phi = 2\pi \delta u/\lambda. \tag{1}$$

It implies that wavelength variations $\delta\lambda/\lambda$ can be described as phase gradients $d\phi/dx$. Pomeau and Manneville [5] established that usually the phase is governed by a diffusion equation. Experimental confirmations of this equation have been given by various groups and among others by Wesfreid and Croquette [6] in a Rayleigh-Bénard experiment. Then, Cross and Brand on a theoretical point of view, and Wu and Andereck on a Taylor-Couette system [7] studied the phase-diffusion mechanism of wavy vortex flow. Then Roth and Lücke investigated the effect of boundaries on the phase dynamics of patterns [7]. All of these mechanisms have been reviewed by Brand [8].

Recently, on the printer's instability, Fourtune, Rappel, and Rabaud [9] have observed a divergence of the phase-diffusion coefficient D in the vicinity of a secondary bifurcation of the pattern called parity-breaking bifurcation. They have interpreted this behavior by a generalization of the phase-diffusion equation proposed by Coullet, Goldstein, and Gunaratne [10], in which the phase-diffusion equation is coupled with a Ginzburg-Landau equation governing the parity-breaking amplitude. What does this behavior become if we consider other secondary bifurcations encountered in one-dimensional systems? We discuss here the case of an oscillatory bifurcation with wavelength doubling sometimes improperly called an ''optical mode.'' This kind of bifurcation appears in different one-dimensional systems, such as the ''printer's instability'' or directional solidification. More recently, we have reported a similar behavior in a new system that we called the liquid-column array. This structure is formed in the process of pouring a liquid from a horizontal overhang, such as the lowest edge of an inclined plate or the bottom of a horizontal cylinder in which a liquid film is flowing. We have also pointed out other dynamical behaviors including the phase-diffusion processes by forcing the motion of a boundary column anchored on a moving needle (capillary contact). Here we investigate quantitatively this dynamics and especially the coupling between phase diffusion and the optical mode.

II. EXPERIMENT

Our experiment consisted of a horizontal, hollow cylinder (external radius $R=2.5$ cm, length $L=28$ cm as in Ref. [11]) supplied at both ends with liquid (silicon oil, 20 cP), at a constant rate q. Owing to a thin slot placed in the upper side of the cylinder, the liquid overflows, runs over the external sides, and accumulates below the cylinder where a Rayleigh-Taylor instability occurs. Depending on the flow rate, different flowing regimes can be observed. Increasing the flow rate, we have identified in succession [12] an array of pendant drops, an array of liquid columns, and a liquid sheet of triangular shape that is hanging below the cylinder. For a large range of flow rate (typically 5–25 g/s), the array of liquid columns is obtained with a well-defined periodicity λ. An example of this pattern is reproduced in Fig. 1. It turns out that λ is usually of order ten times the capillary length l_c with $l_c=(\gamma/\rho g)^{1/2}$ (γ denotes surface tension, ρ mass density, and g gravity, and $l_c \approx 1$ mm for liquid-gas interfaces). Its mean value can be continuously modified by imposing the position of two extreme columns by means of two horizontal needles in capillary contact with the column meniscus [11]

*Present address: Service de Physique de l'Etat Condensé du Commissariat à l'Energie Atomique, Centre d'Etudes de Saclay, F-91191 Gif-sur-Yvette Cedex, France.

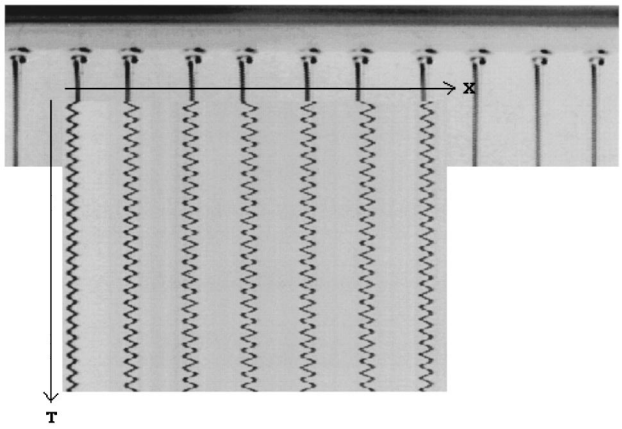

FIG. 1. Array of liquid columns observed below a horizontal cylinder along which a liquid is flowing from top to bottom at a constant rate. Inset: space-time diagram of the array of liquid columns for fixed boundary conditions (optical mode).

(we recall that each extreme column follows the needle motion).

Different dynamical behaviors of the liquid-column array are obtained by varying the wavelength λ or the flow rate q, both playing the role of control parameters. The phase diagram is reproduced in Fig. 2. A wavelength compression leads to coalescence phenomena between columns while a strong dilation leads to nucleation of cells. For moderate wavelength dilations, an oscillatory state is observed in which each column oscillates as a whole, its motion out of phase with that of its nearest neighbors. To follow the columns' motions, we have recorded a line of the digitized picture taken by a video camera and stored at constant time intervals. The line is horizontal and close to the bottom of the cylinder. Thus, we obtain spatiotemporal diagrams such as the one presented in Fig. 1, which gives the $(x-t)$ trajectories of the columns. This regime, called the optical mode, appears for an imposed value of the wavelength higher than a critical value (Fig. 1).

We have plotted in Figs. 3(a) and 3(b) the amplitude and frequency of the oscillations versus the distance to threshold $\varepsilon=(\lambda-\lambda_c)/\lambda_c$ for different values of the flow rate q. The obtained variations reveal a supercritical Hopf bifurcation

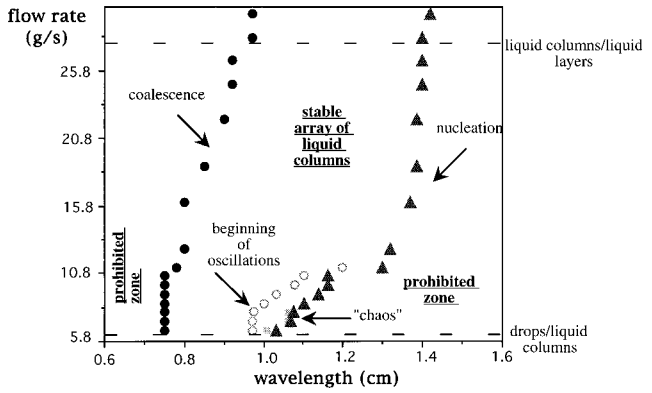

FIG. 2. Phase diagram (q,λ) that shows the stability range of the different dynamic state of the array (q is the global flow rate for the array of 24 liquid columns obtained for the overflowing of a 28-cm horizontal cylinder).

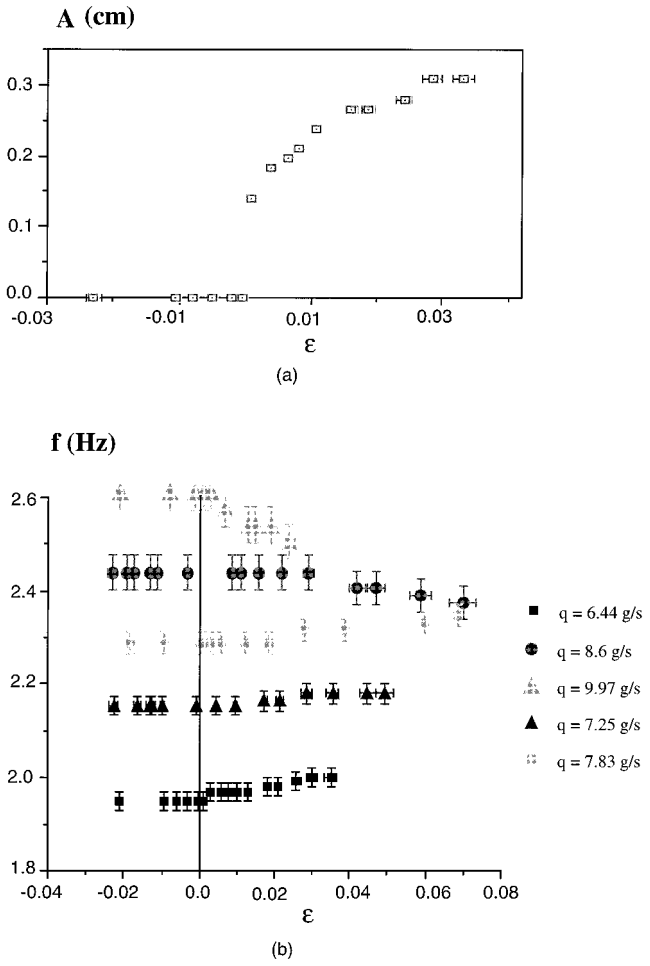

FIG. 3. (a) Amplitude of the oscillations of the columns vs the distance to threshold $\varepsilon=(\lambda-\lambda_c)/\lambda_c$ for $q=6.44$ g/s. (b) Frequency of the oscillations of the columns vs the distance to threshold $\varepsilon=(\lambda-\lambda_c)/\lambda_c$ for different values of the flow rate q.

that confirms previous investigations on lower numbers of oscillating columns [11]. We note that in the range of flow rate [7–10 g/s] the frequency does not depend on ε, which suggests that the motion of the columns is isochronic (i.e., harmonic oscillations).

Time-dependant perturbations can also be achieved by imposing moving boundary conditions on an extreme column, where the needle in contact with this column is slaved to a frequency generator. More precisely, the position of one of the boundary columns is fixed, while the other one oscillates following a law of the kind $x=x_0\cos(2\pi ft)$, where x is the horizontal direction. A phase-diffusion behavior is observed for low forcing amplitude and at low frequency [Fig. 4(a)]. Indeed, the perturbation diffuses in the structure and is progressively damped. When the forcing amplitude increases, the diffusive regime is replaced [11,12] by a propagative regime with dilation wave emissions [Fig. 4(c)]. These waves are characterized by a motion of a group of cells in a direction opposite to the propagation of its boundaries. We have plotted in Fig. 5, the domain of existence of each regime in the plane (f,Ve), $Ve=2\pi fx_0$ being the maximal excitation velocity. In this figure we see that Ve should be higher than a critical velocity to launch the dilation waves. Finally, for velocities larger than a second threshold,

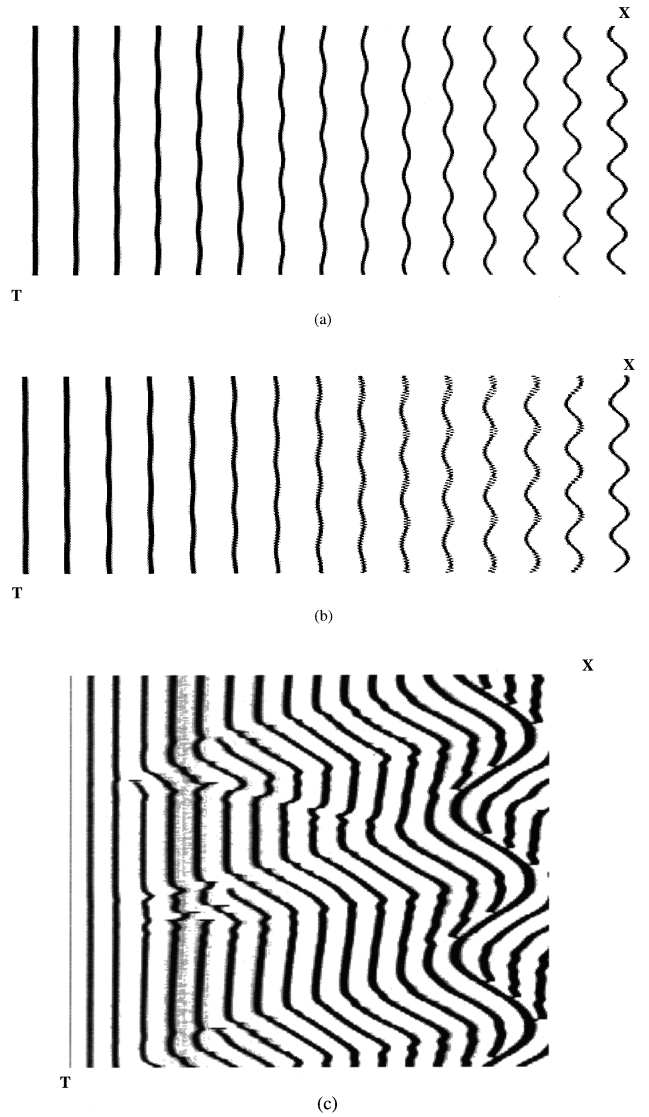

FIG. 4. Space-time diagram of the array of liquid columns with a moving boundary condition following a sinusoidal law $x = x_0 \cos(2\pi f t)$ with $0.1\ \text{cm} < x_0 < 0.5\ \text{cm}$; $f = 0{,}1$ Hz at $q = 7.3$ g/s. X is the position and T is the time that runs toward the bottom. (a) Before the appearance of the optical mode. (b) In the presence of the optical mode. (c) Propagative regime with dilation waves emissions ($x_0 > 0.5$ cm).

we observe only nucleations and coalescences of cells with no propagation anymore.

We now focus the study on the phase dynamics. If we come back to the space-time diagram presented in Fig. 4(a) (low values of x_0 and f), we can see a damping of the oscillations, with a progressive temporal phase shift when x increases. The local amplitude of the forced oscillation $A(x)$ and the local value of the temporal phase shift $\psi(x)$ are plotted as a function of the distance x to the moving boundary [Figs. 6(a) and 6(b)]. In both cases, the linear behavior attests to a phase-diffusion mechanism governed by the following diffusion equation (2) in which D is the phase-diffusion coefficient:

$$\frac{\partial \varphi}{\partial t} = D \frac{\partial^2 \varphi}{\partial x^2}. \tag{2}$$

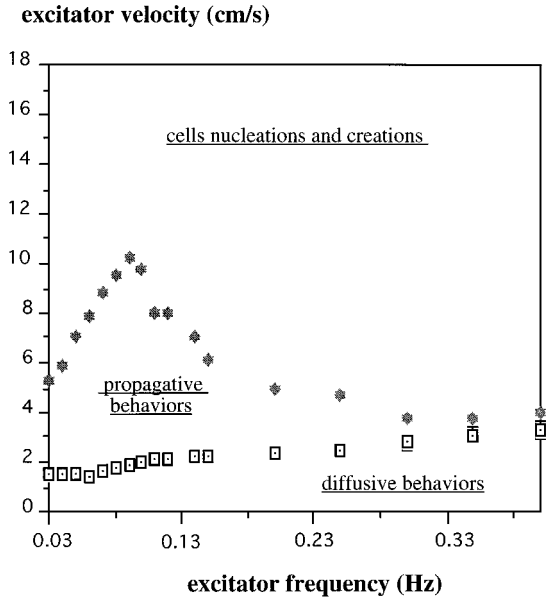

FIG. 5. Different behaviors observed with a moving boundary condition (sinusoidal) at a given flow rate ($q = 7$ g/s).

The solution for Eq. (2) is

$$\varphi(x,t) = \varphi_0 \exp(-\alpha x)\exp[i(\omega t - \beta x)], \tag{3}$$

with

$$\alpha = \beta = \sqrt{\frac{\omega}{2D}}. \tag{4}$$

The experimental results for α and β are presented in Fig. 6(c). These are in agreement with Eq. (3), which confirms the phase-diffusion analysis. These expressions allowed us to perform measurements of the diffusion constant D [12]. Usu-

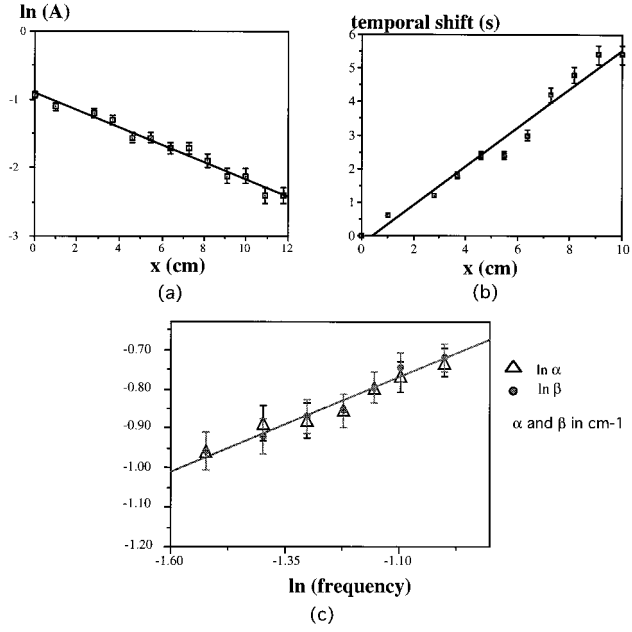

FIG. 6. (a) Spatial dependence of the force amplitude. (b) Spatial dependence of the temporal shift. (c) α and β evolution for $q = 6.88$ g/s; $x_0 = 0.5$ cm.

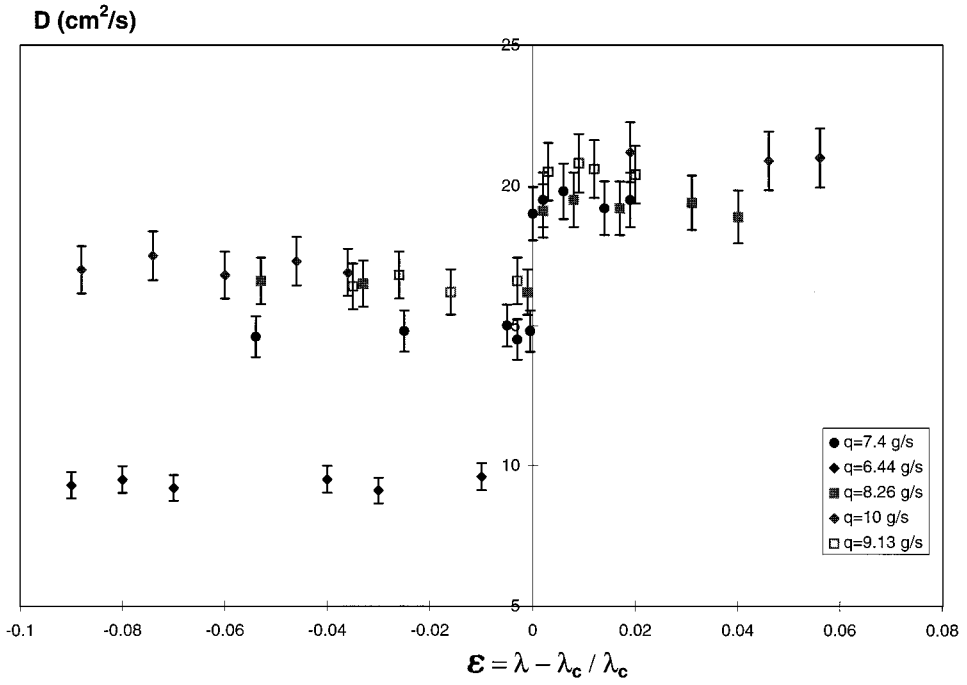

FIG. 7. Phase-diffusion coefficient D evolution at different flow rates (q) with $\varepsilon=\lambda-\lambda_c/\lambda_c$. λ_c is the critical wavelength at the optical-mode appearance.

ally, the obtained values are of the order 10–20 cm^2/s, which compared to the viscosity of the oil (0.2 cm^2/s) are one hundred times higher. We have improved these first measurements by focusing our attention on the dependence of D upon the mean wavelength λ. Indeed, the position of one boundary column is fixed while the other follows a sinusoidal law. In that way, we are able to impose the mean uniform wavelength between the two boundary columns λ. For wavelength values higher than a critical value, the optical mode (high frequency) is coupled with the phase-diffusion mechanism (low frequency) [Fig. 4(b)]. In this case, we determined D by using the central position (half sum of the two extreme positions) of each column to extract the local amplitude of the forced oscillations. The results obtained in four experiments at different flow rates are presented in Fig. 7. It turns out that for a given flow rate, D is constant before the optical-mode appearance and jumps to a new value when the coupling between the optical mode and the phase-diffusion mechanism appears. On the other hand, as is shown in Fig. 8, the constant value of D before the optical-mode appearance increases with the flow rate and reaches a saturation value. After the appearance of the optical mode, D is a constant whatever the flow rate. This behavior differs from that observed with other cellular systems. We can mention, for example, the case of the printer's instability, where $D(\lambda)$ exhibits an Eckhaus scenario when one increases λ for low capillary numbers. On the other hand, for capillary numbers higher than a critical value, a divergence of the coefficient D is observed for increasing wavelength [9]. The same behavior was observed by Misbah [13] in numerical simulations of directional solidification in liquid crystals. Indeed, concerning our system, the array of liquid columns exhibits neither Eckhaus scenario at low flow rates nor divergence at high flow rates, in the range of parameters that we can explore.

III. MODELIZATION OF THE PHASE-DIFFUSION COEFFICIENT JUMP

To explain the previous behavior obtained for the phase-diffusion coefficient, we consider two coupled phase and amplitude equations of the Coullet-Ioss type [14]. This analytical treatment confirms this jump of D when the coupling between the phase-diffusion mechanism and the optical mode appears.

The one-dimensional periodic pattern is described by the even function $U_0(x+\varphi)$ that should describe the shape of the interface. In our case, this pattern bifurcates to an oscillatory state through a Hopf bifurcation characterized by a temporal pulsation $\omega=2\pi f$. In the vicinity of this bifurca-

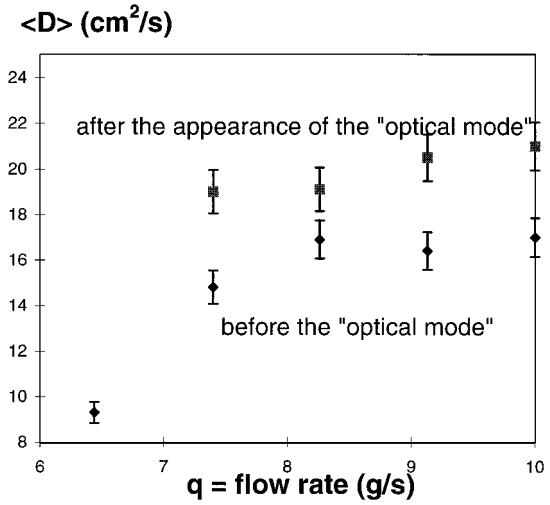

FIG. 8. Phase-diffusion coefficient average $\langle D\rangle$ evolution vs flow rate (q) (below) and after the optical threshold.

tion, the pattern can be described by U as

$$U(x,t,\varphi,A)=U_0(x+\varphi)+\exp(i\omega t)A(x,t)\xi(x+\varphi)+\text{c.c.}, \tag{5}$$

where $\xi(x+\varphi)$ is periodic in x and corresponds to the most unstable mode at the threshold and A is the complex amplitude of the bifurcated solution (optical mode) [14]. So, U depends on the two quantities A and φ, which are supposed to vary slowly in space and time. The dynamics of U is then governed by these quantities, A and φ, which obey two coupled equations obtained by symmetry arguments [15]. These two coupled equations that describe the dynamics of the phase φ and of A are

$$\partial_t A=\mu A+D_A(1+i\alpha)\frac{\partial^2 A}{\partial x^2}-(1+i\beta)|A|^2A - (\gamma+i\delta)\frac{\partial\varphi}{\partial x}A, \tag{6a}$$

$$\partial_t\varphi=D\frac{\partial^2\varphi}{\partial x^2}+i\eta\left(\frac{\partial A}{\partial x}\overline{A}-\frac{\partial\overline{A}}{\partial x}A\right)+\xi\frac{\partial|A|^2}{\partial x}. \tag{6b}$$

All the parameters α, β, γ, δ, η, ξ, and μ are real. μ is a control parameter that has the same destabilization effect as the phase gradient. D is the phase-diffusion coefficient, and D_A is another diffusion coefficient associated with the amplitude A. In view of the frequency measurements presented in Fig. 3(b), we have allowed that $\beta=0$, and for simplicity we have assumed that $\beta=\delta=\xi=0$.

Now we compare two states. The first one is the base state just before the optical-mode appearance ($\mu<0$) characterized by $A=0$. The temporal decrease of a phase modulation defined as $\exp(iQx)\exp(\sigma t)$ will lead to $\sigma=-DQ^2$, where D is the diffusion coefficient with no optical mode. The second state is the one obtained just above the optical-mode threshold ($\mu>0$), where A differs from zero. More precisely, the stationary state that represents a uniform optical mode is defined by the system

$$0=\mu A-|A|^2A, \tag{7a}$$

$$A=\rho_0 e^{i\psi},\qquad \rho_0=\sqrt{\mu},$$

$$\varphi=0,\qquad \psi=\text{const}=0. \tag{7b}$$

We consider the following perturbation:

$$A=\sqrt{\mu}[1+\chi],$$

$$\varphi\neq 0,\qquad \psi\neq 0. \tag{8}$$

Therefore, we have to deal with three coupling variables: the amplitude variation χ, the temporal phase of the oscillations ψ, and the spatial phase of the cellular structure φ. The damping of a phase modulation $\exp(iQx)\exp(\sigma t)$ will give us the effective diffusion coefficient $\tilde{D}$ in the presence of the optical mode by the relationship $\sigma=-\tilde{D}Q^2$. The linear form of our system becomes

$$\begin{pmatrix}\chi_t\\ \psi_t\\ \varphi_t\end{pmatrix}=\begin{pmatrix}-2\mu-Q^2D_A & \alpha Q^2D_A & -iQ\gamma\\ -\alpha Q^2D_A & -Q^2D_A-\sigma & 0\\ 0 & -2i\mu\eta Q & -Q^2D\end{pmatrix}\begin{pmatrix}\chi\\ \psi\\ \varphi\end{pmatrix} =M\begin{pmatrix}\chi\\ \psi\\ \varphi\end{pmatrix}. \tag{9}$$

The characteristic polynomial to obtain $\tilde{D}(Q)$ is given by

$$P(Q,\sigma)=-(Q^2D+\sigma)\begin{vmatrix}-2\mu+Q^2D_A+\sigma & -\alpha Q^2D_A\\ \alpha Q^2D_A & Q^2D_A+\sigma\end{vmatrix} +2\mu\eta\alpha Q^4D_A\gamma=0. \tag{10}$$

We simplify the problem again by asuming that for low coupling, D is only slightly modified and $\tilde{D}=D+\delta D$ with $\delta D\ll D$. Neglecting the δDQ^2 terms comparing to the Q^2D ones, we finally obtain $\tilde{D}$

$$\tilde{D}=D+\delta D=D+\frac{\alpha\eta\gamma D_A}{D-D_A}, \tag{11}$$

with δD containing some corrective terms proportional to the coupling coefficients. As announced above, D is modified just above the threshold, in agreement with our experimental data. Its ''jump'' is proportional to the product $\alpha\eta\gamma$ of the coupling coefficients, that couple $|A|$, φ, and ψ.

IV. CONCLUSION

To conclude, we have identified a specific behavior for the phase-diffusion coefficient D in a cellular system. This behavior is unusual here because D does not follow classical scenarios when increasing the pattern wavelength. We find neither Eckhaus behavior nor divergence with the wavelength. D keeps a constant value and jumps to a new different constant value when the wavelength becomes larger than a critical value where the optical mode appears. This behavior has been recovered by an analytical treatment of Coullet-Ioss equations, the jump of D being proportional to a combination of three coupling coefficients. A direct numerical investigation of this effect is under progress.

This unusual behavior of D is intriguing. The fact that D is nearly constant below threshold is reminiscent of the behavior of the oscillatory pulsation ω that is also independent of the mean wavelength. Both observations are consistent with the idea that the interaction between columns could be governed by a harmonic potential (anharmonicity effects should therefore be removed in the model of Ref. [12]). In comparison to other systems, the absence of Eckhaus scenario and of parity-breaking induced divergence could be explained by the occurrence of nucleation and coalescence of cells that occur very easily in this system and may hide these two behaviors.

ACKNOWLEDGMENTS

This work has benefited from a grant from Centre National d'Etudes Spatiales (CNES). We thank J. Lega for valuable discussions.

[1] J. M. Flesselles, A. J. Simon, and A. J. Libchaber, Adv. Phys. **40**, 1 (1991).
[2] F. Daviaud, M. Dubois, and P. Bergé, Europhys. Lett. **9**, 441 (1989).
[3] M. Rabaud, S. Michalland, and Y. Couder, Phys. Rev. Lett. **64**, 184 (1990); L. Pan and J. R. de Bruyn, Phys. Rev. E **49**, 483 (1994).
[4] J. Bechhoefer, A. Simon, A. Libchaber, and P. Oswald, Phys. Rev. A **40**, 2042 (1989); G. Faivre, S. de Cheveigné, C. Guthman, and P. Kurowski, Europhys. Lett. **9**, 779 (1989).
[5] Y. Pomeau and P. Manneville, J. Phys. (France) Lett. **40**, L609 (1979); H. R. Brand, Prog. Theor. Phys. **71**, 1096 (1984); P. Manneville, *Dissipative Structures and Weak Turbulence* (Academic, New York, 1990).
[6] J. E. Wesfreid and V. Croquette, Phys. Rev. Lett. **45**, 634 (1980); I. Mutabazi, J. J. Hegseth, C. D. Andereck, and J. W. Wesfreid, Phys. Rev. A. **38**, 4752 (1988).
[7] M. Wu and C. Andereck, Phys. Rev. A **43**, 2074 (1991); Phys. Fluids A **4**, 2432 (1992); H. Brand and M. C. Cross, Phys. Rev. A **27**, 1237 (1983); M. Lücke and D. Roth, Z. Phys. B **78**, 147 (1990).
[8] H. R. Brand, in *Propagation in Systems Far From Equilibrium*, edited by J. E. Wesfreid *et al.* (Springer-Verlag, Berlin, 1988).
[9] L. Fourtune, W. J. Rappel, and M. Rabaud, Phys. Rev. E **49**, 3576 (1994).
[10] P. Coullet, R. E. Goldstein, and G. H. Gunaratne, Phys. Rev. Lett. **63**, 1954 (1989).
[11] F. Giorgiutti, A. Bleton, L. Limat, and J. E. Wesfreid, Phys. Rev. Lett. **74**, 538 (1995).
[12] F. Giorgiutti and L. Limat, Physica D **103**, 590 (1997); F. Giorgiutti, Ph.D. thesis, Université Paris-6, 1995.
[13] C. Misbah and A. Valence, Phys. Rev. E **49**, 5477 (1994).
[14] F. Daviaud, J. Lega, P. Bergé, P. Coullet, and M. Dubois, Physica D **55**, 287 (1992).
[15] P. Coullet and G. Ioss, Phys. Rev. Lett. **64**, 866 (1990).